

Impact of model 7-perfume molecule accord on the self-assembly of branched mixed-surfactant system as a function of dilution and dipropylene glycol: A neutron scattering study

Kumari, Harshita*¹; Mirzamani, Marzieh¹; Smith, Ed²

¹ James L. Winkle College of Pharmacy, University of Cincinnati, Cincinnati, OH, USA; ² Procter & Gamble, Mason, Cincinnati, OH, USA

* Prof. Harshita Kumari, James L. Winkle College of Pharmacy, 231 Albert Sabin Way, Medical Science Building 3009 C, University of Cincinnati, OH, USA 45267-0514, Tel: +1-513-558-1872, Email: kumariha@ucmail.uc.edu

Abstract

Background: Perfumes and flavors are very essential ingredients that impact consumer perception. The challenge lies in discerning how complex perfume molecules partition within colloidal domains owing to the number of perfume raw materials (PRMs) used in one perfume composition. Herein, we have studied the structure of a mixed-surfactant system comprising a 7-PRM mixture. Specifically, we look at the effect of dilution and dipropylene glycol on the structure of micelle using small-angle neutron scattering/SANS.

Methods: Five samples were prepared each comprising varying percentages of sodium trideceth-2 sulfate (ST2S), cocamidopropyl betaine (CAPB), the cosolvent dipropylene glycol (DPG); citric acid; the 7-PRM perfume accord (phenylethyl alcohol, benzyl acetate, methyl dihydrojasmonate, dihydromercenol, hexylcinnamic aldehyde, linalool, linalyl acetate). Samples were analyzed on SANS.

Results: The addition of DPG showed a decrease in both Ra and Rb of ellipsoidal geometry. The volume of micelle showed a decrease from 68582 Å³ to 52169 Å³; however, the volume fraction remained the same which indicates the presence of more micelles in the presence of DPG. The dilution from 2:1 (Ra=29.34 Å; Rb=15.82 Å) to 5:1 (Ra=42.06 Å; Rb=17.24 Å) shows an increase in micelle size but a decrease in volume fraction suggesting that micelles break down upon dilution and releases perfume.

Conclusion: This study reveals unique structural features for a mixed perfume accord which were not observed earlier when studied singly. The study further reinforces how 7-PRM vs. 3-PRM/12-PRM compares and how trends in their micellar sizes and volumes are dependent on the localization of PRMs within the formulation.

Keywords: sodium trideceth-2 sulfate; linalool; linalyl acetate; small-angle neutron scattering; perfume raw materials (PRM)

Introduction

Fragrances and flavors are essential ingredients in any cosmetic and food product formulation. Not only do they provide improved aesthetics but also hugely impact the consumer perception.¹⁻⁴ Perfumes are composed of several raw ingredients, and they provide various notes to the formulation. The top note lasts for 5-15 minutes, heart note for 20-60 minutes and base note for up to 6 hours. Perfumers perform the tedious task of manipulating varying ingredients to develop specific fragrances. Notably, the partitioning of these ingredients within the formulation impact the physiochemical behavior of the products.^{5,6} Hence, molecular interaction of perfume raw materials (PRMs) with surfactant and hydrotropes/co-solvents influence design and performance of the product.⁶⁻⁸

A wide range of PRMs are available with varying hydrophobicity/hydrophilicity index due to the presence of different alkyl and function groups (esters, phenols, aldehydes, alcohols). Their log P values (octanol/water partitioning coefficient) determine their partitioning and positioning within the micellar regions.^{9,10} The choice of surfactant and type of hydrotrope/cosolvent impacts the solubility of the PRMs and partitioning. Specifically, the highly polar short-chain alcohols assist improve the solubility in water. Hydrotropes could modify dielectric constant, hydrogen bonding with water and cohesive energy density, which allows for appropriate partitioning of PRMs and release. Most studies reported in the literature involve use of single or binary perfume molecules which do not accurately capture the performance of final products.²¹ The challenge lies in discerning how the complex PRM mixture impacts the colloidal domains within a formulation and how they are released upon dilution that mimics rinse-off scenarios of products, such as, body washes. In this study, we have studied the structure of a mixed-surfactant system comprising a 7-PRM mixture. Specifically, we look at the effect of

dilution and dipropylene glycol on the structure of micelle using small-angle neutron scattering/SANS to mimic rinse-off behavior of formulations and to study the effect of hydrotropes on colloidal domains.

Materials and Methods

Four samples (D-5-1, A-5-1, F-2-1, F-5-1) were prepared each comprising varying percentages of sodium trideceth-2 sulfate (ST2S); cocamidopropyl betaine (CAPB); the cosolvent dipropylene glycol (DPG); citric acid; and a 7-PRM perfume accord consisting of phenylethyl alcohol, benzyl acetate, methyl dihydrojasmonate, dihydromercenol, hexylcinnamic aldehyde, linalool, and linalyl acetate. A fifth sample (E-5-1) was also prepared comprising of the same materials above, except ST2S was substituted with sodium laureth-3 sulfate (SLE3S) and sodium lauryl sulfate (SLS), and the addition of sodium benzoate and disodium EDTA. This fifth sample was included as a control representing a typical body wash or shampoo formulation with linear-tail surfactants. Each sample contained some amount of water due to the surfactant raw materials, so they were diluted with D₂O to improve the signal-to-noise ratio for the SANS experiments. All materials were provided by Procter & Gamble (Cincinnati, OH). It should be noted that these materials are the same industrial-grade materials used by P&G in product manufacturing. These materials were used so that the results would be more representative of an actual formulation. Table 1 shows the compositions of each sample, while Table 2 shows the composition of the 7 PRM perfume accord. The sample names indicate how much the full strength dilution was diluted, i.e. D-5-1 means that the sample consists of 5:1 D₂O:full-strength D formula. D-5-1 and A-5-1 differ in their DPG content, with 0 wt% DPG vs. 2.1 wt% DPG respectively. F-2-1 and F-5-1 differ in the extent of dilution, with F-5-1 having been diluted to a greater extent.

Table 1: Compositions of each sample, given in terms of wt%.

Material	D-5-1 (wt%)	A-5-1 (wt%)	E-5-1 (wt%)	F-2-1 (wt%)	F-5-1 (wt%)
Sodium trideceth-2 sulfate	5.732	5.733	--	11.915	5.957
Sodium laureth-3 sulfate	--	--	1.137	--	--
Sodium lauryl sulfate	--	--	0.437	--	--
Cocamidopropyl betaine	0.988	0.987	0.175	2.051	1.026

Dipropylene glycol	0.000	2.067	--	4.293	2.147
Citric acid	0.107	0.107	0.026	0.220	0.110
Sodium benzoate	--	--	0.044	--	--
EDTA (2 Na)	--	--	0.018	--	--
Sodium chloride	--	--	0.413	--	--
Phenylethyl alcohol (perfume)	0.159	0.159	0.020	0.202	0.101
Benzyl acetate (perfume)	0.195	0.195	0.025	0.248	0.124
Methyl dihydrojasmonate (perfume)	0.294	0.294	0.038	0.373	0.187
Dihydromyrcenol (perfume)	0.203	0.203	0.026	0.258	0.129
Hexylcinnamic aldehyde (perfume)	0.281	0.281	0.036	0.357	0.178
Linalool (perfume)	0.201	0.201	0.026	0.255	0.127
Linalyl acetate (perfume)	0.255	0.255	0.033	0.324	0.162
Water	8.252	6.186	14.214	12.838	6.419
Deuterated water	83.333	83.333	83.333	66.667	83.334

Table 2: Composition of the 7 PRM perfume accord.

Material (CAS#)	Structure	Content (wt%)	Mol. Weight (g/mol)	$c \log P$
Benzyl Acetate (140-11-4)		12.3	150.18	1.7
Dihydro Myrcenol (18479-58-8)		12.8	156.3	3.08
Phenyl Ethyl Alcohol (60-12-8)		10.0	122.17	1.32
Linalyl Acetate (115-95-7)		16.1	196.286	3.93
Linalool (78-70-6)		12.6	154.2493 2	2.97

Methyl Dihydro Jasmonate (24851-98-7)		18.5	226.3	3.01
Hexyl Cinnamic Aldehyde (101-86-0)		17.7	216.3	4.3

Each sample was loaded into a titanium cell holder with quartz windows set 1 mm apart, for a 1 mm sample thickness. SANS study was conducted at Oak Ridge National Laboratory, which was set at two different detector distances and one neutron wavelength to achieve the desired q-range. The low-q SDD (sample to detector distance) was 5.2 m, while the wavelength was 5 Å. For high-q, the SDD was 1.2 m with a 5 Å neutron wavelength. These settings gave a q-range of $0.006752 \text{ \AA}^{-1}$ to 0.5455 \AA^{-1} with the scattering vector $q = \frac{4\pi}{\lambda} \sin \frac{\theta}{2}$ and θ being the scattering angle. The resulting data from each instrument configuration was reduced by correcting for background scattering, detector resolution, and instrument geometry, then set to absolute scale using the beam transmission, and performing a circular average using the reduction macros in Igor Pro.¹¹ The data from both configurations for each sample were then combined to form a single data set spanning the entire q-range.

The data was analyzed using the uniform ellipsoid¹² form factor and the rescaled mean spherical approximation (MSA)^{13,14} structure factor using SasView version 5.0.3.¹⁵ A polydispersity term was included for R_b (semi-minor axis, perpendicular to axis of rotation R_a). The decoupling approximation¹⁶ was used to correct for errors in the structure factor calculation caused by polydispersity and non-spherical particle geometry.

Results

The SANS data were analyzed in SasView version 5.0.3 using the Uniform Ellipsoid form factor with the rescaled MSA structure factor model. Overlays of the scattering data and the

model fits are shown in Figure 1, while Table 3 shows the fitting results. The Uniform Ellipsoid form factor model is averaged over all orientations of particles and is normalized by the particle volume, V_{ell} . The aggregation number was calculated from the total molar surfactant concentration and the position of the maximum peak intensity (Q_{max}).¹⁷ The average distance between the micelles, D , was calculated using the equation

$$D = 6.8559/(Q_{max} - 0.0094).$$

The aggregation number N_{agg} was then calculated from D and the surfactant concentration with the equation

$$N_{agg} = \left(\frac{D\sqrt{2}}{10^8}\right)^3 \frac{N_A \times C}{4000}$$

where N_A is Avogadro's number and C is the molar surfactant concentration. The fractional charge was then obtained by dividing the charge determined from the SANS fits by the aggregation number.

The results show that the micellar structures in all samples formed prolate ellipsoidal geometry, including sample E-5-1. The addition of DPG from 0 wt% (D-5-1) to approximately 2 wt% (A-5-1) decreases both R_a and R_b , with R_a being greatly affected compared to R_b . The micelle volume decreased from 68582 Å³ to 52169 Å³; however, the volume fraction increased slightly which indicates the presence of more micelles in the presence of DPG. The effective radius, R_{eff} , which indicates how much space the particle fills on average if it were spherical, including the head groups which do not contrast strongly with the surrounding bulk solvent, did not change significantly as DPG was added. The aggregation number dropped as well, corresponding to an increase in the fractional charge (Table 3).

Increasing the extent of dilution from 2:1 (F-2-1) to 5:1 (F-5-1) causes an increase in micelle size due to R_a elongating by almost 50% and R_b also lengthening slightly. At the same time, the volume fraction drops by more than 50%, suggesting that micelles break down upon dilution and releases perfume. R_{eff} drops to a similar size after the samples were diluted as after DPG was added, despite R_a and R_b increasing. The aggregation number decreased as the system was diluted, coupled with a large increase in the fractional charge.

Table 3: Fitting results of the model to the data.

Sample	Volume Fraction	R_a (Å)	R_b (Å)	R_{eff} (Å)	Aggregation Number	Fractional Charge
D-5-1	0.11	44.61	19.16	28.27	115.26	0.12
A-5-1	0.12	36.06	18.58	28.40	96.55	0.15
E-5-1	0.03	37.10	21.35	26.43	117.34	0.09
F-2-1	0.27	29.34	15.82	33.12	117.00	0.04
F-5-1	0.12	42.06	17.24	26.95	94.80	0.13

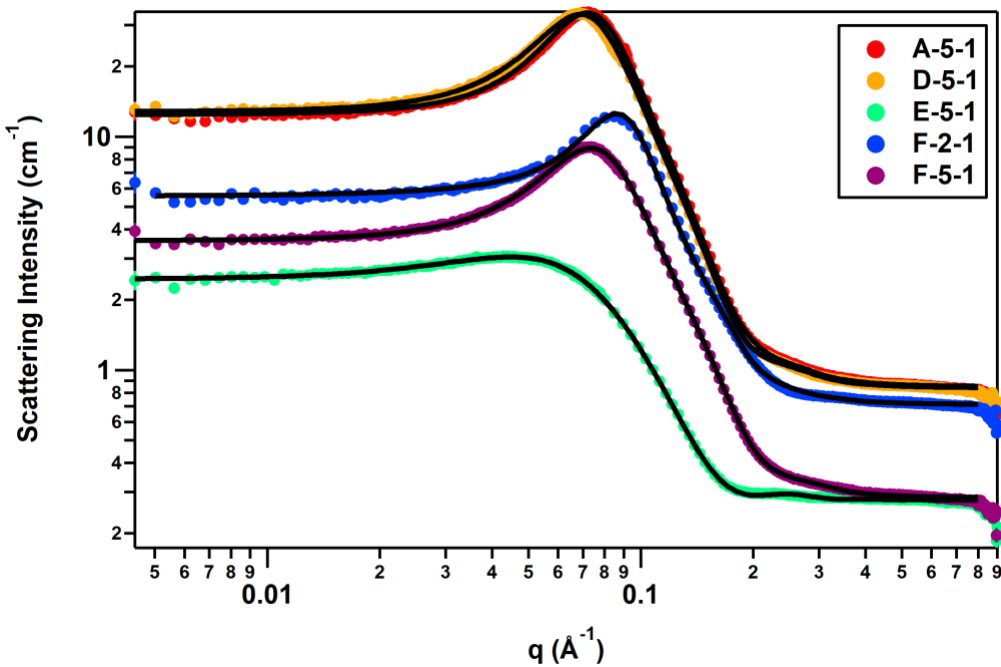


Figure 1: Overlay of the SANS data and their fits. Solid black lines are the fits to the data using the uniform ellipsoid form factor and screen coulomb structure factor. The data curves and fits for E-5-1, F-2-1, and F-5-1 were not offset, while the curves and fits for A-5-1 and D-5-1 were offset by a factor of 3 for clarity and ease of comparing the effect of DPG (A-5-1 vs. D-5-1) and dilution (F-2-1 vs. F-5-1).

Discussion.

We earlier reported a 3-PRM¹⁸ and 12-PRM¹⁹ accord and the effect of dilution on mixed branched chain ST2S/CAPB surfactant self-assembly. The 3-PRM accord¹⁸ was a subset of 7-PRM accord comprising of phenylethylalcohol, dihydromercenol and hexyl cinnamic aldehyde, whereas 12-PRM¹⁹ accord comprised of 3-PRM ingredients (phenylethylalcohol, dihydromercenol and hexyl cinnamic aldehyde) along with benzyl acetate, pyronol, β -Ionone, Undecavertol, Ambronat, Heliotropin, γ -decalactone, methyl dihydrojasmonate and hexamethylindanopyran. In case of 3-PRM paper, we created a phase diagram study and specifically studied the no-

PRM vs. transition vs. microemulsion area. Fewer components in 3-PRM, allowed us to track the positioning of PRMs within the colloidal domain. ^1H NMR (nuclear magnetic resonance) spectroscopy revealed that the 3-PRMs' were preferentially located within the core of micelles. It indicated that a strong intermolecular interaction exists between the three PRMs molecules and how these interactions had a strong influence on their location within the micellar core.¹⁸ For the more complex 12-PRM accord, discerning the positioning of PRMs through ^1H NMR was challenging due to several overlapping chemical peaks. Instead, we studied the effect of dilution at varying water concentrations ranging from 35 to 90 wt%. An increase in ellipsoidal micellar volume was observed for ≥ 50 wt% water with an increase in perfume content. Interestingly a much higher rate of volume increase was observed for ≥ 70 wt% water concentrations.¹⁹

Unlike these accords, the current study involves a 7-PRM mixture which comprises of linalool and linalyl acetate (along with 3-PRM ingredients, benzyl acetate and methyl dihydrojasmonate). Linalool is a acyclic monoterpene known to not only have excellent fragrance but is also used as a calming agent and hence used for both cosmetic and therapeutic effects. Both linalool and its ester form, linalyl acetate, are the main constituents of the lavender oil. The odor of linalool is described as floral, citric, sweet and fresh, while the odor of linalyl acetate described as floral, sweet, citric, minty and slightly caraway-like.²⁰

The only other two studies reported comprising of linalool were those with Penfold wherein he observed lamellar phases using SANS.^{21, 22} In the first study of 2008, Penfold and co-workers studied the role of single PRMs with varying hydrophilicities on the self-assembly of non-ionic dodecaethylene monodecyl ether ($\text{C}_{12}\text{EO}_{12}$) and mixed surfactant mixture of $\text{C}_{12}\text{EO}_{12}$ and cationic dialkyl chain surfactant dihexadecyl dimethyl ammonium bromide (DHDAB). They studied perfume solubilization in order of increasing hydrophobicity: phenyl ethanol (PE), rose oxide (RO), limonene (LM), linalool (LL) and dihydrogen mercenol (DHM). While the hydrophilic PE solubilized/partitioned predominantly at the hydrophilic/hydrophobic interface of $\text{C}_{12}\text{EO}_{12}$ and mixed $\text{C}_{12}\text{EO}_{12}$ /DHDAB mixtures, the hydrophobic perfumes (RO to DHM) partitioned in hydrophobic core of micelles. In addition, the more hydrophobic LL and DHM promoted substantial growth of micelles.²²

In a separate study in 2013, Penfold reported the effect of adding linalool and phenylethanol on the solution structure of sodium dodecyl 6-benzene sulfonate using SANS.²¹ Over most of the concentration-composition space, they observed primarily lamellar or vesicular structures. At lower concentrations of linalool, Penfold observed monodispersed nanovesicles which were significantly different from the lamellar phase.²¹

Herein, the 7-PRM accord for the mixed-surfactant system reveals the presence of an ellipsoidal geometry. While exact positioning of PRMs was difficult to discern through ¹H NMR due to overlapping peaks, notable structural observations were noticed. The volume of the 7-PRM accord with DPG is 1.5 times lower than that of a 12-PRM¹⁹ accord at comparable dilution and perfume-to-surfactant ratio. Similarly, a 1.3 times lower micellar volume is observed for a 7-PRM accord than a 12-PRM¹⁹ accord. This observation is consistent with our earlier reported localization of PRMs within the micellar core.¹⁸ The negligible change in R_{eff} with addition of DPG means that the micelles still took up the same amount of space despite being smaller as DPG was added, which would suggest that the head group region of the micelles now makes up a larger portion of the micelle. This change in the head group region of the micelles would not be visible to SANS due to the poor contrast between the head group and the surrounding solvent.

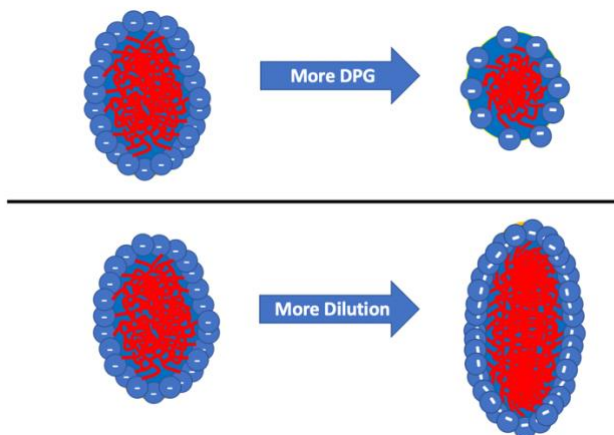


Figure 2: Schematic of the effect of DPG concentration and dilution on micellar size

The Ra for linear SLE3S/CAPB surfactant was comparatively lower than branched ST2S/CAPB surfactant systems at no DPG (D-5-1) and 86 % water concentrations (F-5-1) but the R_{eff} overall was comparable due a longer R_b for linear surfactant system (Figure 2).

This demonstrates the effect of tail length on the shape of micelle. Interestingly, the fractional charge for the linear surfactant (E-5-1) was lower than that of the branched surfactant system (D-5-1) despite comparable aggregation numbers due to more effective screening of charges at the surface of linear surfactant micelle. In a separate study, we have performed a calibration study wherein we have systematically investigated the effect of DPG and surfactant concentration on perfume release (12-PRM) on mixed-micellar systems of branched-chain ST2S/CAPB and linear-chain SLE1S/CAPB through combined GC-MS (gas chromatography mass spectroscopy), SANS and statistical analyses.²³

The micellar size, specifically Ra values for 7-PRM accord is higher than those observed for 12 PRM¹⁹ and 3 PRM¹⁸ accords. This could be attributed to the presence of linalool and linalyl acetate in the 7-PRM accord. In addition, a significant increase in fractional charges is observed as a function of dilution which was not effectively captured for a more complex 12-PRM¹⁹ accord. Dilution could potentially cause linalyl acetate to partition into the head group of micelles leading to higher fractional charges.

Conclusion. In conclusion, we report the effect of hydrotropes /DPG and dilution on a branched mixed-surfactant system comprising of a 7-PRM accord. The no-DPG linear versus branched surfactant system is also compared and distinct differences in size and fractional charges are observed. Uniquely, this 7-PRM accord comprises multiple ingredients, especially linalool and linalyl acetate which are otherwise studied singly. Both linalool and linalyl acetate are important ingredients of lavender oil and have usage in both personal care and therapeutic applications. The results suggest unique structural features for a mixed accord which were not observed earlier when studied singly. The study further reinforces how 7-PRM vs. 3-PRM¹⁸ vs. 12 PRM¹⁹ compares and how trends in their micellar sizes and volumes are dependent on the localization of PRMs within the formulation. Multiple PRM accords are difficult yet very important to study owing to their vast application in cosmetic industry.

Acknowledgments. This work was funded by Procter & Gamble, Mason, Cincinnati, OH.

Conflict of Interest Statement. NONE.

References.

- (1) Sowndhararajan, K.; Kim, S. (2016) Influence of Fragrances on Human Psychophysiological Activity: With Special Reference to Human Electroencephalographic Response. *Scientia Pharmaceutica*, 84: 724-751.
- (2) Annett, J. M. (1996) Olfactory Memory: A Case Study in Cognitive Psychology. *The Journal of Psychology*, 130: 309-319.
- (3) Bargh, J. A. (2002) Losing Consciousness: Automatic Influences on Consumer Judgment, Behavior, and Motivation. *Journal of Consumer Research*, 29, 280-285.
- (4) White, T. L.; Treisman, M. A. (1997) comparison of the encoding of content and order in olfactory memory and in memory for visually presented verbal materials. *British Journal of Psychology*, 88: 459-472.
- (5) Fischer, E.; Fieber, W.; Navarro, C.; Sommer, H.; Benczédi, D.; Velazco, M. I.; Schönhoff, M. (2008) Partitioning and Localization of Fragrances in Surfactant Mixed Micelles. *Journal of Surfactants and Detergents* 12: 73-84.
- (6) Qu, Q.; Tucker, E.; Christian, S. D. (2003) *Journal of Inclusion Phenomena and Macrocyclic Chemistry* 45: 83-88.
- (7) Fan, Y.; Tang, H.; Strand, R.; Wang, Y. (2016) Modulation of partition and localization of perfume molecules in sodium dodecyl sulfate micelles. *Soft Matter* 12: 219-227.
- (8) Grillo, I.; Morfin, I.; Prévost, S. (2018) Structural Characterization of Pluronic Micelles Swollen with Perfume Molecules. *Langmuir* 34: 13395-13408.
- (9) Fieber, W.; Frank, S.; Herrero, C. (2018) Competition between surfactants and apolar fragrances in micelle cores. *Colloids and Surfaces A: Physicochemical and Engineering Aspects* 539: 310-318.
- (10) Zhao, G.-X.; Li, X.-G. (1991) Solubilization of n-octane and n-octanol by a mixed aqueous solution of cationic-anionic surfactants. *Journal of Colloid and Interface Science* 144: 185-190.
- (11) Kline, S. R. (2006) Reduction and Analysis of SANS and USANS Data Using IGOR Pro. *Journal of Applied Crystallography* 39: 895-900.
- (12) Feigin, L. A.; Svergun, D. I.: *Structure Analysis by Small-Angle X-Ray and Neutron Scattering*; Plenum Press: New York, 1987.
- (13) Hayter, J. B.; Penfold, J. (1981) An analytic structure factor for macroion solutions. *Molecular Physics* 42: 109-118.
- (14) Hansen, J.-P.; Hayter, J. B. (1982) A rescaled MSA structure factor for dilute charged colloidal dispersions. *Molecular Physics* 46: 651-656.
- (15) Doucet, M.; Cho, J. H.; Alina, G.; Attala, Z.; Bakker, J.; Bouwman, W.; Butler, P.; Campbell, K.; Cooper-Benun, T.; Durniak, C.; Forster, L.; Gonzales, M.; Heenan, R.; Jackson, A.; King, S.; Kienzle, P.; Krzywon, J.; Nielsen, T.; O'Driscoll, L.; Potrzebowski, W.; Prescott, S.; Ferraz Leal, R.; Rozyczko, P.; Snow, T.; Washington, A. SasView version 5.0.3. *Zenodo* **2020**.
- (16) Hayter, J. B.; Penfold, J. (1983) Determination of micelle structure and charge by neutron small-angle scattering. *Colloid & Polymer Science* 261: 1022-1030.

- (17) Prasad, C. D.; Singh, H. N.; Goyal, P. S.; Rao, K. S. (1993) Structural Transitions of CTAB Micelles in the Presence of n-Octylamine: A Small Angle Neutron Scattering Study. *Journal of Colloid and Interface Science* 155: 415-419.
- (18) Mirzamani, M.; Dawn, A.; Aswal, V. K.; Jones, R. L.; Smith, E. D.; Kumari, H. (2021) Investigating the effect of a simplified perfume accord and dilution on the formation of mixed-surfactant microemulsions. *RSC Advances* 11: 25858-25866.
- (19) Mirzamani, M.; Reeder, R. C.; Jarus, C.; Aswal, V.; Hammouda, B.; Jones, R. L.; Smith, E. D.; Kumari, H. (2022) Effects of a Multicomponent Perfume Accord and Dilution on the Formation of ST2S/CAPB Mixed-Surfactant Microemulsions. *Langmuir*. 4, 1334–1347.
- (20) d'Acampora Zellner, B., Casilli, A., Dugo, P., Dugo, G., and Mondello, L.. (2007) Odour fingerprint acquisition by means of comprehensive two-dimensional gas chromatography-olfactometry and comprehensive two-dimensional gas chromatography/mass spectrometry. *J. Chromatogr. A* 1141: 279–286.
- (21) Bradbury, R.; Penfold, J.; Thomas, R. K.; Tucker, I. M.; Petkov, J. T.; Jones, C.; Grillo, I. (2013) Impact of model perfume molecules on the self-assembly of anionic surfactant sodium dodecyl 6-benzyl sulfonate. *Langmuir* 29: 3234–3245.
- (22) Penfold, J.; Tucker, I.; Green, A.; Grainger, D.; Jones, C.; Ford, G.; Roberts, C.; Hubbard, J.; Petkov, J.; Thomas, R.K.; Grillo, I. (2008) Impact of model perfumes on surfactant and mixed surfactant self-assembly. *Langmuir* 24: 12209–12220.
- (23) Mirzamani, M.; Flickinger, M.; Kharb, S.; Jones, R. L.; Ananthapadmanabhan, K.; Smith, E.; Kumari, H. (2022). Investigating the effect of dipropylene glycol and mixed-surfactant concentrations on perfume release. *Colloids and Surfaces A: Physicochemical and Engineering Aspect Accepted, In Press. Manuscript ID: COLSUA-D-22-01960R2*

Supplemental Information

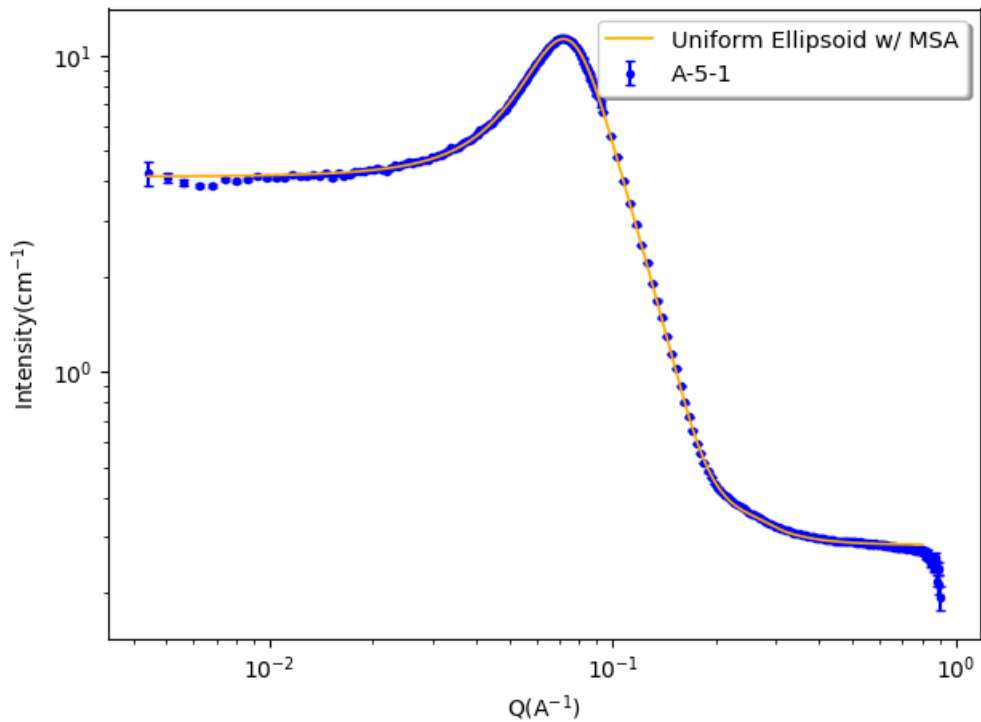
Small-angle Neutron Scattering (SANS) Analysis

Scattering length densities (SLDs) of each surfactant + perfume system and its respective solvent system (a mixture consisting of DPG if relevant, citric acid, D₂O to improve the SANS signal-to-noise ratio and H₂O from the surfactant) used in modeling the data are shown below in Table S1. The SLDs were calculated using NIST's neutron activation and scattering calculator at <https://www.ncnr.nist.gov/resources/activation/>. Weighted averages of every component expected to be in the surfactant self-assembly (ST2S, CAPB, and the 7 PRMs linalool, linalyl acetate, benzyl acetate, methyl dihydrojasmonate, dihydromyrcenol, hexyl cinnamic aldehyde, and phenylethyl alcohol) and in the solvent phase (D₂O, H₂O, citric acid, and DPG) were calculated. One sample, E-5-1, had a somewhat different composition, but the calculations of the continuous and dispersed phase SLDs were the same. The weighted averages, molecular formulae, and densities of each component in the dispersed phase and the solvent phase were entered into the NIST activation calculator as shown to obtain the reported particle and solvent SLDs.

Code	Entry for Particle SLD	Particle SLD	Entry for Solvent SLD	Solvent SLD
A-5-1	69.01%wt C17H35NaO6S@1.1 // 11.87%wt C19H38N2O3@1.04 // 1.91%wt C8H10O@1.02 // 2.35%wt C9O2H10@1.054 // 3.54%wt C13H22O3@0.998 // 2.44%wt C10H20O@0.784 // 3.38%wt C15H20O@0.95 // 2.42%wt C10H18O@0.863 // C12H20O2@0.895	4.34E-7	6.75%wt H2O@0.998 // 90.88%wt D2O@1.107 // 2.25%wt C6H14O3@1.023 // C6H8O7@1.542	5.71E-07
D-5-1	68.99%wt C17H35NaO6S@1.1 // 11.89%wt C19H38N2O3@1.04 // 1.91%wt C8H10O@1.02 // 2.35%wt C9O2H10@1.054 // 3.54%wt C13H22O3@0.998 // 2.44%wt C10H20O@0.784 // 3.38%wt C15H20O@0.95 // 2.41%wt C10H18O@0.863 // C12H20O2@0.895	4.34E-07	9%wt H2O@0.998 // 90.88%wt D2O@1.107 // C6H8O7@1.542	5.69E-06
E-5-1	8.98%wt C19H38N2O3@1.04 // 58.22%wt C18H37NaO7S@1.152 // 22.39%wt C12H25NaSO4@1.01 // 1.04%wt C8H10O@1.02 // 1.28%wt C9O2H10@1.054 // 1.93%wt C13H22O3@0.998 // 1.33%wt C10H20O@0.784 // 1.84%wt C15H20O@0.95 // 1.32%wt C10H18O@0.863 // C12H20O2@0.895	4.41E-07	14.5%wt H2O@0.998 // 84.99%wt D2O@1.107 // 0.04%wt C7H5NaO2@1.497 // 0.02%wt C10H14N2Na2O8@0.86 // 0.42%wt NaCl@2.17 // C6H8O7@1.542	5.27E-06

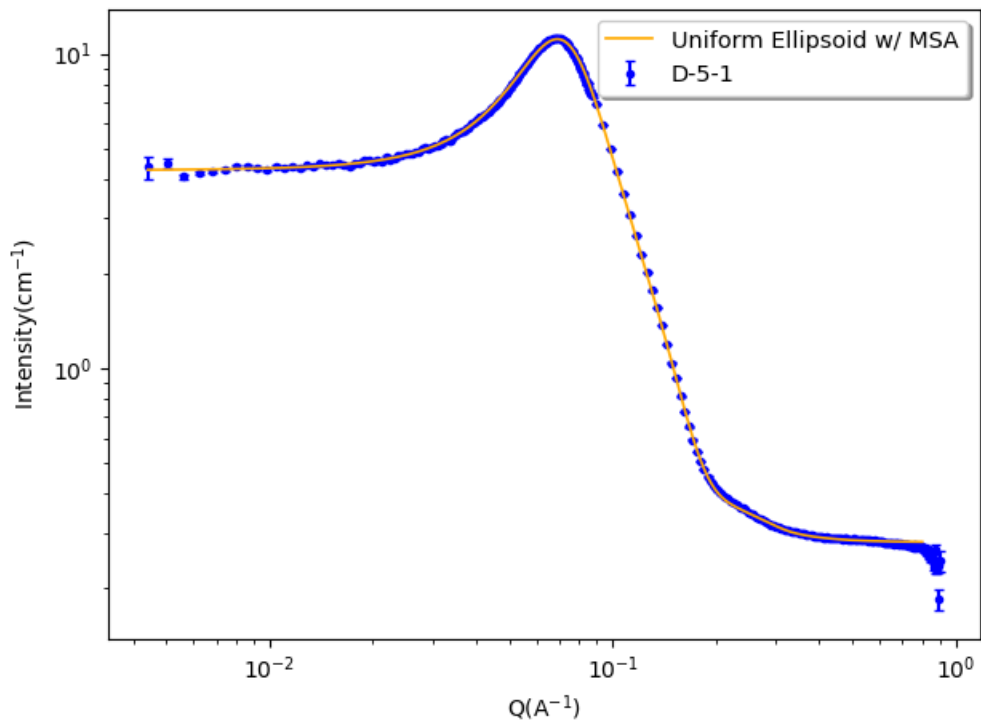
F-2-1	74.55%wt C17H35NaO6S@1.1 // 12.83%wt C19H38N2O3@1.04 // 1.26%wt C8H10O@1.02 // 1.55%wt C9O2H10@1.054 // 2.34%wt C13H22O3@0.998 // 1.61%wt C10H20O@0.784 // 2.23%wt C15H20O@0.95 // 1.59%wt C10H18O@0.863 // C12H20O2@0.895	4.20E-07	15.28%wt H2O@0.998 // 79.35%wt D2O@1.107 // 5.11%wt C6H14O3@1.023 // C6H8O7@1.542	4.88E-06
F-5-1	74.55%wt C17H35NaO6S@1.1 // 12.83%wt C19H38N2O3@1.04 // 1.26%wt C8H10O@1.02 // 1.55%wt C9O2H10@1.054 // 2.34%wt C13H22O3@0.998 // 1.61%wt C10H20O@0.784 // 2.23%wt C15H20O@0.95 // 1.59%wt C10H18O@0.863 // C12H20O2@0.895	4.20E-07	6.98%wt H2O@0.998 // 90.57%wt D2O@1.107 // 2.33%wt C6H14O3@1.023 // C6H8O7@1.542	5.69E-06

A-5-1 (Uniform Ellipsoid with MSA Model)



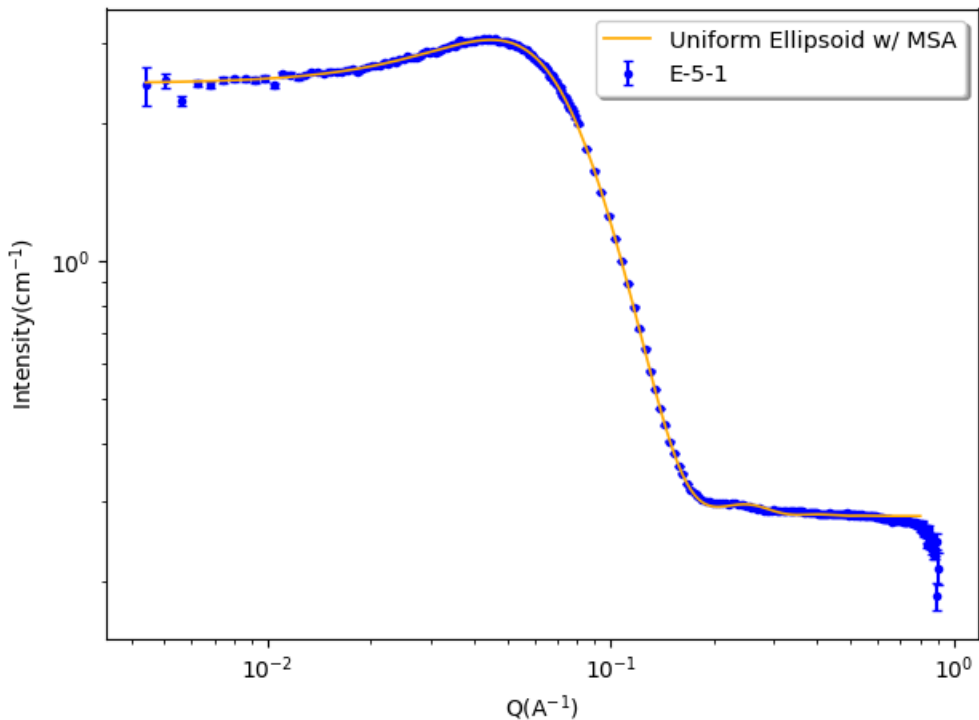
Parameter	Result	\pm	Error
Background	0.28	\pm	5.49E-05
R_a (Å)	36.06	\pm	8.73E-02
R_b (Å)	18.58	\pm	7.90E-03
Polydispersity R_b	0.20	\pm	5.51E-04
R_{eff} (Å)	28.40	\pm	1.17E-02
Volume Fraction	0.12	\pm	5.36E-05
Charge	14.12	\pm	2.59E-02
Salt Conc. (M)	0	\pm	0
Fit Range	0.004	$< Q <$	0.8
Sqrt(χ^2)			4.5502

D-5-1 (Uniform Ellipsoid with MSA Model)



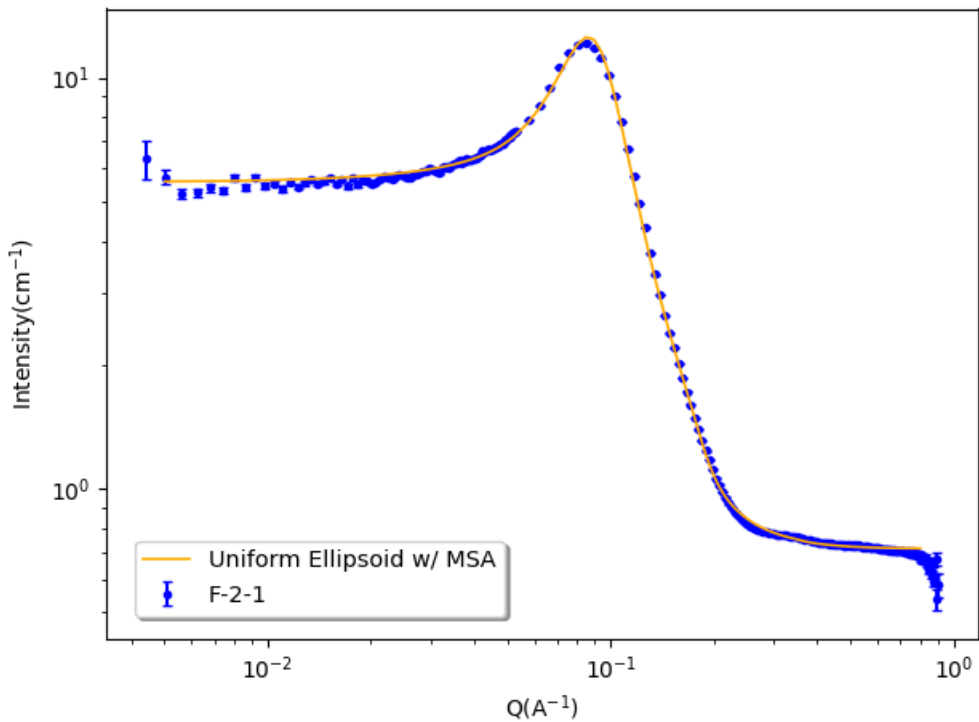
Parameter	Result	±	Error
Background	0.28	±	5.43E-05
R _a (Å)	44.61	±	1.43E-01
R _b (Å)	19.16	±	8.28E-03
Polydispersity R _b	0.17	±	5.26E-04
R _{eff} (Å)	28.27	±	1.08E-02
Volume Fraction	0.11	±	5.69E-05
Charge	13.44	±	2.91E-02
Salt Conc. (M)	0	±	0
Fit Range	0.004 < Q < 0.8		
Sqrt(χ^2)			4.3349

E-5-1 (Uniform Ellipsoid with MSA Model)



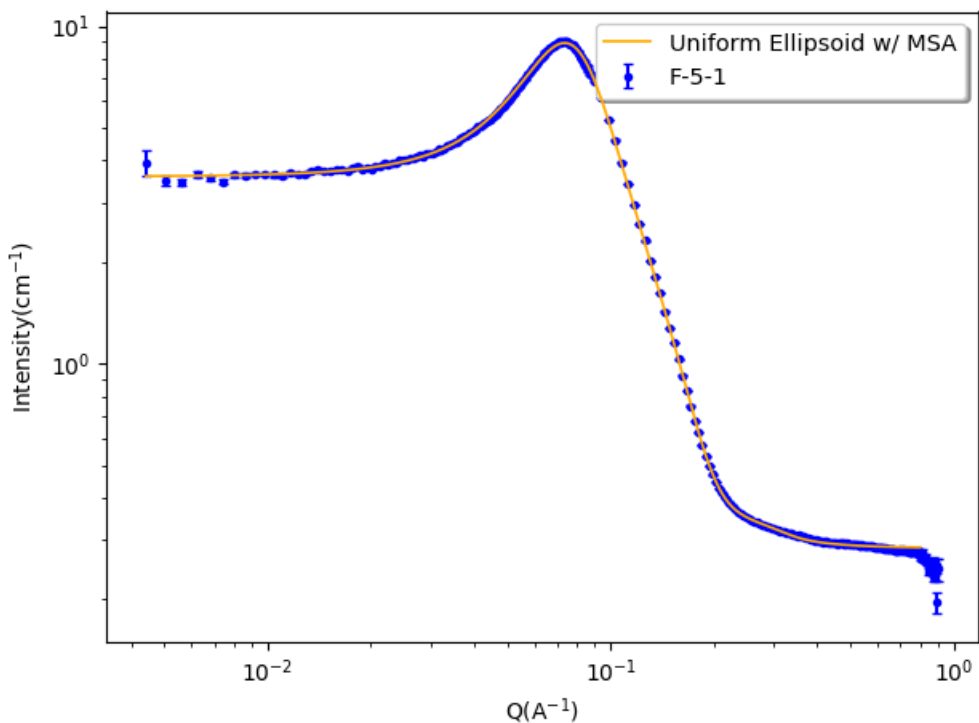
Parameter	Result	±	Error
Background	0.28	±	5.08E-05
$R_a (\text{\AA})$	37.10	±	2.02E-01
$R_b (\text{\AA})$	21.35	±	1.37E-02
Polydispersity R_b	0	±	0
$R_{\text{eff}} (\text{\AA})$	26.43	±	2.17E-01
Volume Fraction	0.03	±	2.78E-05
Charge	10.11	±	4.14E-01
Salt Conc. (M)	0.02	±	1.27E-03
Fit Range	0.004	< Q <	0.8
Sqrt(χ^2)			4.3102

F-2-1 (Uniform Ellipsoid with MSA Model)



Parameter	Result	±	Error
Background	0.71	±	1.21E-04
R_a (Å)	29.34	±	7.49E-02
R_b (Å)	15.82	±	1.24E-02
Polydispersity R_b	0.24	±	1.09E-03
R_{eff} (Å)	33.12	±	2.12E-02
Volume Fraction	0.27	±	1.21E-04
Charge	4.62	±	1.40E-01
Salt Conc. (M)	0	±	0
Fit Range	0.005 < Q < 0.8		
Sqrt(χ²)			8.2554

F-5-1 (Uniform Ellipsoid with MSA Model)



Parameter	Result	±	Error
Background	0.28	±	5.57E-05
R_a (Å)	42.06	±	1.50E-01
R_b (Å)	17.24	±	8.30E-03
Polydispersity R_b	0.18	±	5.91E-04
R_{eff} (Å)	26.95	±	1.22E-02
Volume Fraction	0.12	±	6.02E-05
Charge	11.90	±	2.83E-02
Salt Conc. (M)	0	±	0
Fit Range	0.004	< Q <	0.8
Sqrt(χ²)			4.1275